

Minimizing Alkali Usage Through Ultrasound Treatment of Oil Palm Empty Fruit Bunch (OPEFB) Fiber Reinforced Poly(Lactic) Acid Composites

John Olabode Akindoyo, Mohammad Dalour Hossen Beg*, Suriati Binti Ghazali,
Muhammad Remanul Islam

Faculty of Chemical and Natural Resources Engineering, Universiti Malaysia Pahang
Lebuhraya Tun Razak, Gambang 26300, Kuantan, Malaysia.

blessebode@ymail.com; dhbeg@yahoo.com*; suriati@ump.edu.my; remanraju@yahoo.com.

*Correspondence: M.D.H. Beg, email: dhbeg@yahoo.com; Phone: +6019504590; Fax: +6095492816)

Abstract -Removal of the non-cellulosic components of natural fibers with minimum damage to the fibers had been one of the challenges to natural fiber reinforced polymer composites. Alkali treatment had been one of the very efficient means of fiber treatment. However, environmental concerns make it expedient to always reduce the concentration of alkali for any fiber treatment as much as possible. In this study, ultrasonic treatment in an alkali medium of low concentration was used to modify the surface of oil palm empty fruit bunch (OPEFB) fibers. Surface morphology of fibers due to treatment was studied by scanning electron microscopy (SEM) while its structural changes were studied by Fourier transforms infrared spectroscopy (FTIR) and X-ray diffraction (XRD). Composites were prepared from oil palm empty fruit bunch fiber and poly(lactic) acid (PLA) through extrusion followed by injection moulding. Composite characterization was done by mechanical testing such as tensile, flexural and impact, structural analysis was done by XRD and thermogravimetric analysis (TGA) was also to investigate composite thermal stability. Result showed that the treatment of OPEFB fibers with ultrasound produced composites with highly desirable properties.

Keywords: Ultrasound; oil palm empty fruit bunch fiber; composites; interfacial adhesion

1. Introduction

The use of cellulose natural fibers in more sophisticated forms like in composite fabrication had recently gained increased attention. This is especially because they can function as readily available, cheap, environmentally friendly and renewable alternatives to synthetic and non-renewable fibers in composites (Zhou et al., 2011). Natural fiber reinforced thermoplastic composites are also experiencing enormous growth based on their many desirable properties which include reasonable stiffness and strength, reduced abrasiveness and light weight. Preference to natural fiber in composites bores down mainly to its nontoxic, combustible, renewable, light weight, nonabrasive and biodegradable properties (Islam, Beg, Gupta, & Mina, 2013; Moshiul Alam, Beg, Reddy Prasad, Khan, & Mina, 2012). However, natural fiber reinforced polymer composites often present composites with weak interface as a result of the poor interfacial interaction between surfaces of the hydrophilic fibers and the hydrophobic polymer matrices. But chemical and physical treatments can effectively modify the surface of the fibers by cleaning the surface as well as increase its surface roughness (Huda, Drzal, Mohanty, & Misra, 2008; Mohanty, Verma, Nayak, & Tripathy, 2004; Petersson, Kvien, & Oksman, 2007).

Treatment of fibers would either activate the hydroxyl groups of the fiber cellulose, or incorporate new functional groups to the fiber surface which can effectively bond with the matrix (Khalid, Salmiaton, Chuah, Ratnam, & Choong, 2008). Treatment of fibers had led to fabrication of property enhanced composites from natural fibers like kenaf, bamboo, jute, ramie, flax, coir, wood and oil palm fibers. It was noted however that most of the conventional fiber treatment methods like mercerization, acetylation, coupling agents, acrylation and peroxide treatment often make use of organic solvents. This therefore led to the release of hazardous substances into the environment (Zhou et al., 2011).

A non-conventional environmental friendly alternative is the use of ultrasound energy for fiber treatment. Ultrasound is one extreme way of creating an unusual chemical environment within a solution by the generation of some little cavities which are capable of enlarging and imploding. This process therefore generates enormous heat as series of ultrasonic waves are allowed to pass through the solution (Muthukumaran, Kentish, Stevens, & Ashokkumar, 2006). Ultrasound treatment being a modern environmentally-friendly treatment technique had been widely accepted in separation technology. Recently, it has been noted that ultrasound treatment of natural fibers offers several advantages for fiber purification (Islam et al., 2013; Moshiul Alam et al., 2012). Few among these are better purification with minimum alkali concentration, minimum exposure time in the reaction chamber, lower treatment temperature and better mechanical strength due to the lower degree of damage (Moshiul Alam et al., 2012).

Ultrasound can efficiently enhance the mechanical and physical properties of the fibers and their reinforced composites by the application of ultrasonic energy to the fiber. This would lead to controlled residual compressive stress, fiber refinement and fiber size reduction, which is a good prerequisite for enhanced mechanical strength of composites (Goriparthi, Suman, & Mohan Rao, 2012; Meon, Othman, Husain, Remeli, & Syawal, 2012). Although the effect of ultrasound is both physical and chemical, the chemical effect is usually more pronounced as well as influences the observable changes to the fiber than the physical effect. However, this chemical effect often comes through physical processes on the fiber especially in the liquid medium in which case there is possibility of formation, expansion and implosion of gaseous and vaporous cavities (Aimin, Hongwei, Gang, Guohui, & Wenzhi, 2005; Muthukumaran et al., 2006). This physical process often leads to long term chemical effect through the use of cavitation from the ultrasonic wave to agitate the fiber in the liquid medium. Fiber agitation leads to production of high forces on strictly adhered debris on the fiber surface thereby thoroughly removing all traces of impurity tightly adhering or embedded unto the fiber surface, bringing about a rougher surface morphology (Moshiul Alam et al., 2012).

Several reports had shown that oil palm empty fruit bunch fiber, among several other natural fibers had been used to reinforce polymers in different applications and at varying degrees. Notable among these are incorporation of natural fibers into thermoplastics like PLA. However, a vast majority of these studies show that there is apparently poor adhesion between the fiber and the PLA matrix interface, hence the need for further modifications to improve the surface interaction of OPEFB fibers and PLA matrix (Bledzki, Jaszkiwicz, & Scherzer, 2009; Huda et al., 2008; Petersson et al., 2007).

In this study, ultrasound treatment was carried out on oil palm empty fruit bunch (OPEFB) fibers in alkali medium containing 2% (w/v) NaOH. Composites were fabricated from untreated and treated OPEFB fibers and comparisons were drawn between the composites and pure PLA. Interfacial adhesion between fiber and matrix was investigated with respect to fiber surface modification. Surface morphology, functional groups analysis and structural analysis of the untreated and treated fibers were investigated. Mechanical properties, structural properties and thermal stability of composites were also investigated.

2. Materials and Methods

2.1. Materials

The oil palm empty fruit bunch (OPEFB) fibers used for this study was collected as waste raw materials from LKPP oil palm Sdn. Bhd., Kuantan, Malaysia. The polymer matrix which is thermoplastic poly(lactic) acid was supplied by Unic Technology Ltd, China. It is a Natureworks Ingeo™ Biopolymer 3051D grades, with a melt flow index of 30-40g / 10 min (190°C/2.16kg), density of 1.24 g/cm³ and melting temperature between 160-170°C. Other chemicals used include analytical grade sodium hydroxide and acetic acid which were procured from Merck, Germany.

2.2. Methods

Fiber treatment

The raw oil palm empty fruit bunch fibers collected from the oil palm industry contained several impurities ranging from sand particle, stones, palm kernel, mud, ash and other debris. The fibers were

washed in water flow to remove these adhering particles, after which it was left to dry in air for 3 days. Dried fibers were cut using plastic crusher machine and sieved with a mechanical sieve shaker to remove ash as well as to obtain uniform size between 2-5 mm. After this, ultrasound treatment of fibers was done by soaking the fibers in 2% (w/v) NaOH solution and placed in ultrasound bath (CREST- ultrasonics) maintained at 90°C and 9 Watts for about 100 min. Optimization of ultrasound working condition was initially carried out as described in literature (Moshiul Alam et al., 2012), while the weight of fiber to solution was kept at 1:20 (w/v) during treatment. After treatment, the OPEFB fibers were washed in distilled water continuously to remove excess alkali. This was continued and few drops of very dilute acetic acid was added until the water no longer show signs of alkalinity i.e. pH of 7 attained, after which the fibers were dried in air for 24 hr and in oven for 8 hr at 70°C.

Composite fabrication

The compounding of poly(lactic) acid (PLA) with untreated and treated OPEFB fibers was done using a twin screw extruder (model - THERMO SCIENTIFIC PRISM EUROLAB-16), fitted with a fixed length pelletizer. Preparation of samples for testing was done by initially drying the pellets in oven at 70°C until it was moulded with an injection moulding machine (model- DR BOY 22M). Temperature parameter for extrusion and injection moulding of samples is presented in Table 1. Composites were fabricated from untreated OPEFB fibers and PLA with 0, 10, 20, 30 and 40 wt% fiber loading. Mechanical testing showed that 30 wt% fiber produced the highest mechanical properties. Composite was therefore prepared for treated fiber and PLA maintaining the 30 wt% fiber content. Samples which were prepared for further analysis are untreated OPEFB fibers (UF), ultrasound-alkali treated OPEFB fibers (TF), pure poly(lactic) acid (PLA), untreated OPEFB/PLA composites (UFC) and ultrasound-alkali treated OPEFB/PLA composites (TFC).

Table. 1. Operation parameters for Extrusion moulding (EM) and Injection moulding (IM) of OPEFB and PLA composites

EM Conditions		IM Conditions	
Temperature Profile:		Temperature Profile:	
Zone	Temp.	Section	Temp.
Feeding zone:	110 °C	Feeding section:	160 °C
Mixing zone:	175-185 °C	Compression section:	175-185 °C
Metering zone:	190 °C	Metering section:	190 °C
Die:	185 °C	Nozzle:	180-185 °C
		Mould:	25-30 °C
Screw speed:	100-110 rpm	Screw speed:	155 rpm
Torque:	55-60 (%)	Screw position:	28.5 mm
		Injection time:	0.45 sec
		Cooling time:	25 sec

Mechanical testing of composite

Tensile testing of composites

Tensile test samples were prepared according to ASTM 638- 08: Standard Test Method for Tensile Properties of Plastics. Testing was carried out using a Shimadzu universal tensile machine (model- AG-1) fitted with load cell of 5 KN, operated at crosshead speed of 10 mm min⁻¹ on tensile samples with 65 mm gauge length. Seven samples for each batch were tested out of which five replicates specimens were presented as an average of tested specimens.

Charpy impact testing of composites

Impact testing was conducted according to EN ISO 179 Plastics – Determination of Charpy impact strength. Testing was carried out on rectangular impact test samples with dimension as 55 x 3.3 x 10 using a Ray-Ran universal pendulum impact tester with an impact velocity of 3.04 m/s and hammer weight of 0.168 kg. Prior to testing, a Ray-Ran motorised notching cutter was used to notch test samples to a depth of 1.5 mm. Average of five replicate specimen samples was taken out of seven tested specimens for each composite category.

Three points bend testing of composites

Three points bend test was carried out on test specimens according to ASTM D790-97: Standard. Testing was done using a Shimadzu universal tensile machine (model- AG-1) with static load cell of 5 KN. The dimensions of test sample were 125 x 3.3 x 12 mm. The cross head speed was set at 3 mm min⁻¹ with support kept at 50 mm apart. Testing was done at room temperature. Average of five replicate specimen samples was recorded out of seven tested specimens for each composite category.

Surface morphological analysis (SEM)

The surface morphology of untreated and treated were analysed by a ZEISS, EVO 50 scanning electron microscope. Prior to SEM observation test sample were coated with gold using a vacuum sputter-coater to make them conductive.

Fourier transforms infrared spectroscopy (FTIR) analysis

Fourier transform infrared spectroscopy (FTIR) analysis was done for untreated and treated fibers. This functional group analysis was carried out by a Fourier Transforms Infrared Spectrophotometer (model- THERMO) using the standard KBr technique after which spectrum for each fiber type was taken with the help of OMNIC software.

Structural analysis with XRD

X-ray diffraction analysis was carried out in order to determine the crystalline structure of untreated and treated OPEFB fibers as well as composites. Analysis was done at a scanning speed of 1deg min⁻¹, sampling step of 0.02° and scanning range 3-30°, using an X-ray diffractometer.

Thermogravimetric analysis (TGA)

Thermogravimetric analysis was carried out using a thermogravimetric analyser (TA model- TGA Q500 V6.4). This was done to determine the thermal stability of fiber and composite. Each specimen weighing about 5 ± 2 mg was placed in platinum crucible under a nitrogen atmosphere with a flow rate of 40 mL min⁻¹ to avoid unnecessary oxidation.

3. RESULTS AND DISCUSSION

Morphology of fiber

The SEM images of untreated and treated OPEFB fibers shown in Fig. 1. reveals that the surface of the untreated fiber was smooth and even. This could be due to the presence of cementing substances like lignin, hemicellulose and waxes on the fiber surface. On the other hand, image for the treated fiber reveals uneven and coarse surface with many opened pores. This indicates the effectiveness of ultrasound treatment to remove considerable amount of cementing substances from the fiber surface. Removal of these binding and sizing structures therefore led to increased effective surface area and porosity of the fiber by revealing the pore spaces as seen in Fig. 1(ii). Exposure of the pores spaces also confirm the structural changes that ultrasound treatment had caused to the fiber perhaps by disrupting the hydrogen bonding in the structural framework of the OPEFB fiber. These changes are good incentives for better mechanical interlocking of the fiber with polymer matrix during composite fabrication as reported in literature (Goriparthi et al., 2012; Moshiul Alam et al., 2012).

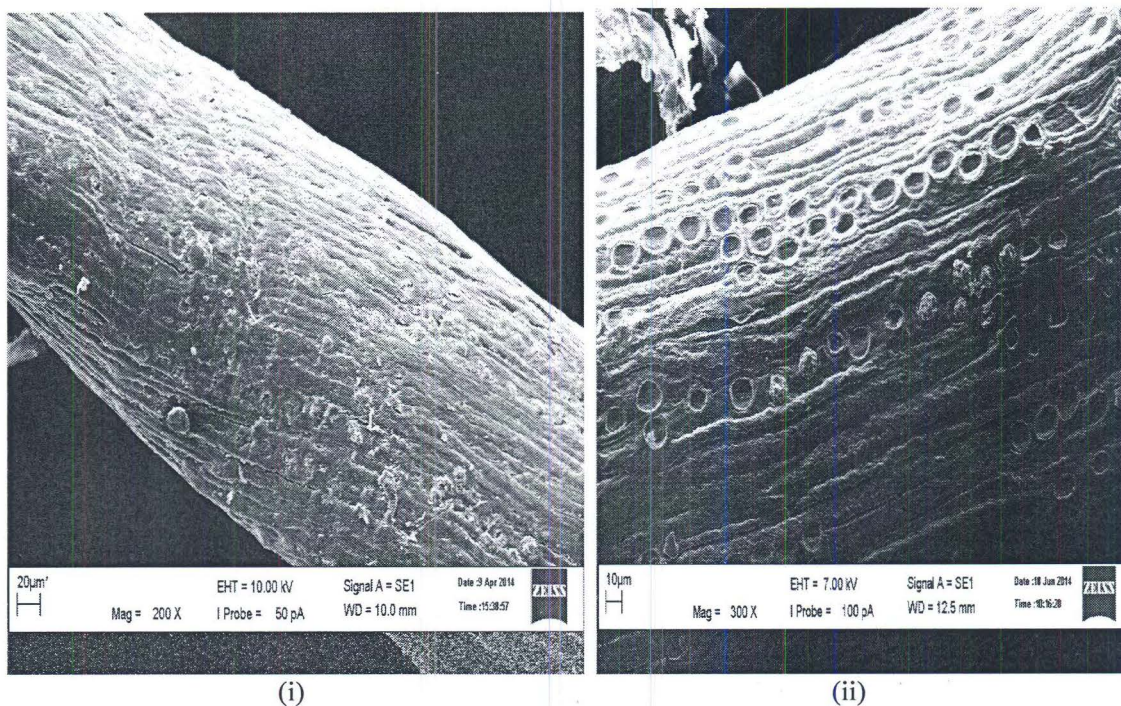


Fig. 1. Surface morphology of OPEFB fiber (i) before and (ii) after treatment with ultrasound in alkali medium.

Fourier transforms infrared spectroscopy (FTIR) analysis

The FTIR spectra of OPEFB fiber before and after treatment are illustrated in Fig. 2. The spectrum for both fiber types looks similar. The region from around $4000\text{-}1900\text{ cm}^{-1}$ does not really provide much needed information. This might be because this region is usually a characteristic of vibrations from -OH and aliphatic C-H stretching of the fiber components (Sun, Tomkinson, & Ye, 2003). The major observed peaks are $3500\text{-}3200\text{ cm}^{-1}$ which represents broad band for stretching vibrations of hydrogen bonded -OH groups. The peak around 2900 cm^{-1} is due to vibrations coming from stretching of the methyl and methylene moieties in cellulose and hemicellulose components of OPEFB fiber. The other region from $1900\text{-}700\text{ cm}^{-1}$ seems to be more informative. The peaks in this region include at 1749 cm^{-1} which represents the stretching of carbonyl (C=O) of ester and carboxylic components of lignin and hemicellulose (Chowdhury, Beg, Khan, & Mina, 2013). The peaks at 1644 cm^{-1} and 1514 cm^{-1} are due to =CH vibrations from aromatic skeletal and -C=C bending in lignin components of the fiber respectively. The peak at 1422 cm^{-1} represents -CH_3 asymmetric and C-H symmetric deformation of fiber lignin. Representations of the C-H stretching in methyl, methylene and methoxy groups of lignin was noticed at 1318 cm^{-1} , whereas aromatic C-H in-plane deformation of lignin is evident at 1034 cm^{-1} . The peak at 1241 cm^{-1} represents asymmetric stretching of -C-O-C- in the β -glycosidic bond of cellulose chain (Moshiul Alam et al., 2012). In general, the major difference between spectrum for untreated and treated OPEFB fiber is the weakening and sharpening of peaks at certain points, as well the disappearance of peaks at some other point. Conspicuous among these is the disappearance of the peak at 1749 cm^{-1} for untreated fiber. This suggests an effective removal of significant portions of the fiber hemicellulose and lignin due to ultrasound and alkali treatment of OPEFB fibers, as reported elsewhere (Moshiul Alam et al., 2012). Also the peak at 1644 cm^{-1} for untreated fiber can be seen to appear at a lower wavelength in treated fiber spectrum, indicating some structural changes to the fiber after treatment with ultrasound and alkali. Structural changes to fibers with respect to fiber treatment were also noticed by other researchers

(Goriparthi et al., 2012; Sgriccia, Hawley, & Misra, 2008). Other observable changes to the spectrum of treated fiber include the reduced absorption intensity and also little upward shifting of the peak at 1422 cm^{-1} . This suggests effective removal of considerable amount hemicellulose and lignin from fibers after treatment as reported elsewhere (Islam et al., 2013). This was further confirmed by the sharpness of the peak at 1318 cm^{-1} for treated fibers. Summary of the observed peaks is presented in Table 2.

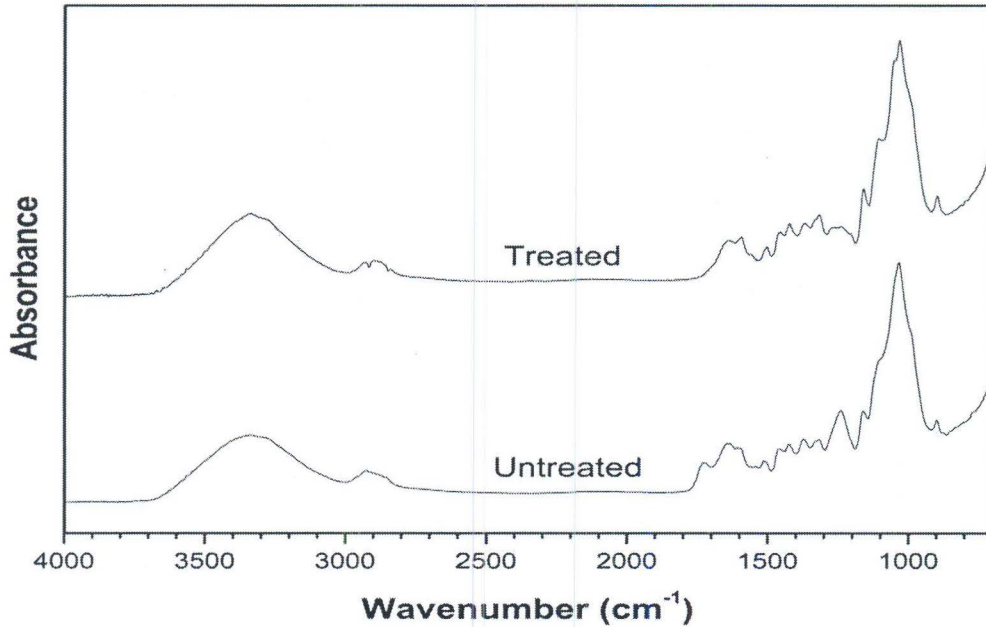


Fig. 2. FTIR spectra of OPEFB fiber before and after treatment

Table 2. Summary of FTIR spectra for untreated and treated OPEFB fibers

Position of bands (cm^{-1})		
Untreated	Treated	Functional group representation
3335	3385	-OH bond structure of cellulose
2924	2922	C-H stretching vibration of cellulose
1749	-	C=O stretching
1644	1595	=CH vibration from aromatic skeletal
1514	1509	-C=C bending in lignin
1422	1424	-CH ₃ asymmetric and C-H symmetric deformation
1318	1317	C-H stretching in methyl, methylene and methoxy groups
1241	1240	-C-O-C- β -glycosidic linkage in cellulose
1034	1031	Aromatic C-H in plane deformation
898	986	Si-O asymmetric stretching

Structural analysis with XRD

The XRD diffractograms of untreated and treated OPEFB fiber as well as the diffractograms for PLA, UFC and TFC are illustrated in Fig. 3i and ii. The conspicuous peaks observed for fibers and the

composites is at $2\theta \approx 22.2^\circ$ and $2\theta \approx 16.2^\circ$ which represent the crystalline and amorphous components of the fiber cellulose respectively. These peaks were analysed and the result is presented in Table 3. For untreated OPEFB fiber, the conspicuous peak at $2\theta = 22.17^\circ$ represents the crystallographic (002) planes of the OPEFB fiber cellulose (Chowdhury et al., 2013). This peak can be seen to shift towards the higher angle after fiber treatment indicating a reduced interplanar spacing of the (002) planes as confirmed by the d-spacing data in Table 3. Moreover, the reduced FWHM value suggests a closer packing of cellulose crystal structure after fiber treatment perhaps due to removal of hemicellulose and lignin from the fiber, causing the cellulose to rearrange and form new chains through hydrogen bonding (Islam et al., 2013; Müller, Laurindo, & Yamashita, 2009). This might be responsible for the increased crystal size and crystallinity of treated fiber perhaps through transcristallinity via hydrogen bonding of OPEFB fiber cellulosic hydroxyl groups as reported elsewhere (Islam et al., 2013).

On the other hand for PLA and OPEFB/PLA composites, comparing the diffractograms in Figure 3ii reveals the diffused peak observed for PLA which is different from the diffractograms of the composites. This diffused peak of PLA indicates a poorly ordered chain with low degree of crystallinity most likely as a result of the rapid cooling process of injection moulding. This similar peak was reported for injection moulded PLA in literature (Moshiul Alam et al., 2012). From Table 3, the crystalline peak position can be seen to be shifted to the higher angle after the incorporation of OPEFB fiber into PLA. This might be due to macro stress effect, leading to a reduced molecular distance as well as reduced amorphous nature of the PLA molecules (Moshiul Alam et al., 2012). Crystallite size and crystallinity of the composites can also be seen to be higher than for pure PLA, with treated fiber composite (TFC) having the highest. This suggests that combined ultrasound and alkali treated OPEFB fibers are capable of acting as nucleating agents for the crystallization of PLA. This also is an indication of improved fiber-matrix interfacial adhesion of ultrasound and alkali treated OPEFB fibers with PLA as reported by other researchers (Lee, Kim, Lee, Kim, & Dorgan, 2009; Pickering, Sawpan, Jayaraman, & Fernyhough, 2011).

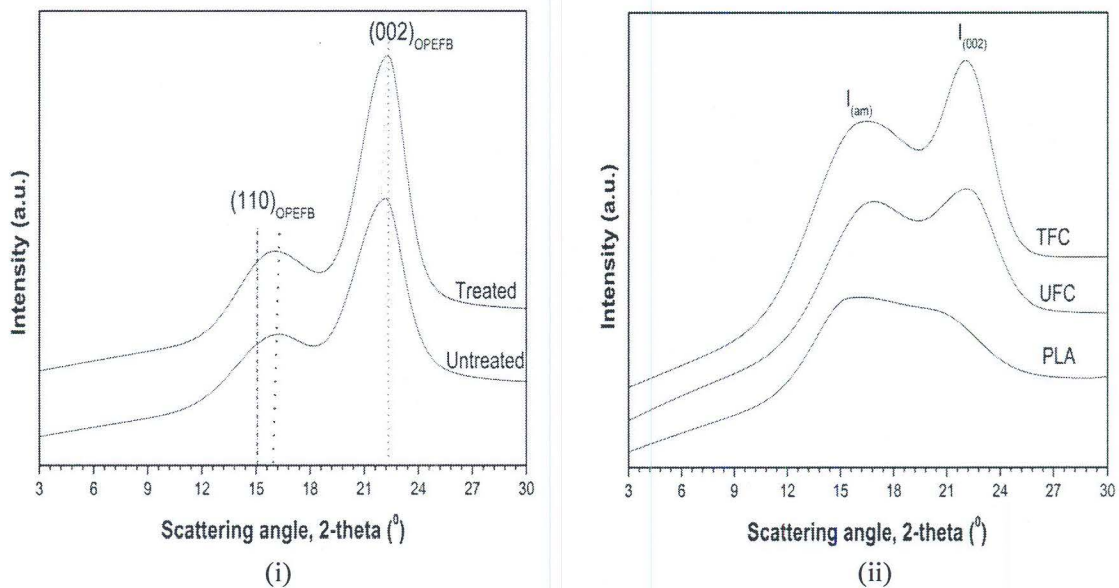


Fig. 3. XRD diffractograms of (i) untreated and treated OPEFB fiber and (ii) pure PLA, untreated OPEFB fiber composite (UFC) and treated OPEFB fiber composite (TFC).

Table 3. Crystalline XRD parameters of untreated OPEFB fiber (UF), treated OPEFB fiber (TF), pure PLA, untreated OPEFB fiber composite (UFC) and treated OPEFB fiber composite.

Parameters	Fiber		Composites		
	UF	TF	PLA	UFC	TFC
Peak position (2 θ)	22.17	22.47	21.20	22.22	22.34
FWHM (2 θ)	3.19	2.63	4.20	3.87	2.96
d (Å)	4.01	3.954	4.19	3.99	3.97
Crystallite size (nm)	26.50	32.20	20.00	21.90	28.60
CrI (%)	40.27	44.17	41.23	44.59	63.44

Mechanical properties of composites

The variation of tensile strength (TS), tensile modulus (TM), flexural strength (FS), flexural modulus (FM) and impact strength (IS) of untreated OPEFB/PLA with fiber loading is presented in Fig. 3i, ii and iii. From Fig. 3i and ii, it can be seen that the TS, TM, FS, and FM all increased as the fiber loading increased up to 30 wt% loading. After 30 wt% fiber loading, these properties can be seen to reduce at 40 wt%. The initial increase in mechanical properties of OPEFB/PLA composites with respect to fiber loading can be attributed to the highly desirable individual mechanical properties of OPEFB fibers as reported elsewhere (Moshiul Alam et al., 2012). Below 30 wt%, the low improvement observed could be as a result of insufficiency quantity as well as uneven distribution of fiber within the matrix, leading to ineffectiveness in stress transfer from the PLA matrix to fibers. The highest values for TS, TM, FS and FM were obtained at 30 wt% fiber loading perhaps due to even distribution of fibers within the matrix at 30 wt% fiber loading, making load transfer between fiber and matrix more efficient. The observed decreases when the fiber loading exceeded 30 wt% could be a result of overloading effect of fiber on the matrix at 40 wt%. Excessive fiber loading might lead to fiber agglomeration within the composite; leading to poor wettability of the fiber by the PLA matrix as well as creation of stress transfer breaks (Islam et al., 2013; Joseph, Joseph, & Thomas, 2006). Fig. 3iii illustrates the effect of fiber loading on IS of untreated OPEFB/PLA composites. The inclusion of fiber into PLA led to an initial drop in IS perhaps due to creation of local stress concentration sites within the composite. The IS can however be seen to increase gradually as the fiber loading increased up to 30 wt%. This suggest that at 30 wt% fiber loading, the fibers can absorb sufficient energy to toughen PLA thereby reducing the effect of shock on the PLA matrix as well as increase the overall shock absorption ability of the composite (Bledzki, Mamun, & Feldmann, 2012; Mamun, Heim, Beg, Kim, & Ahmad, 2013). Above 30 wt% there might have been an excessive amount of fiber within the composite, leading to reduced surface area for redirecting cracks. This suggests that at higher fiber content, there is possibility for micro crack formation at impact points within the composite (Mamun et al., 2013; Wirjosentono, Guritno, & Ismail, 2004). The improvement in properties of OPEFB/PLA composite at 30 wt% fiber loading above pure PLA is 5%, 31%, 19%, 57% and 2% for TS, TM, FS, FM and IS respectively.

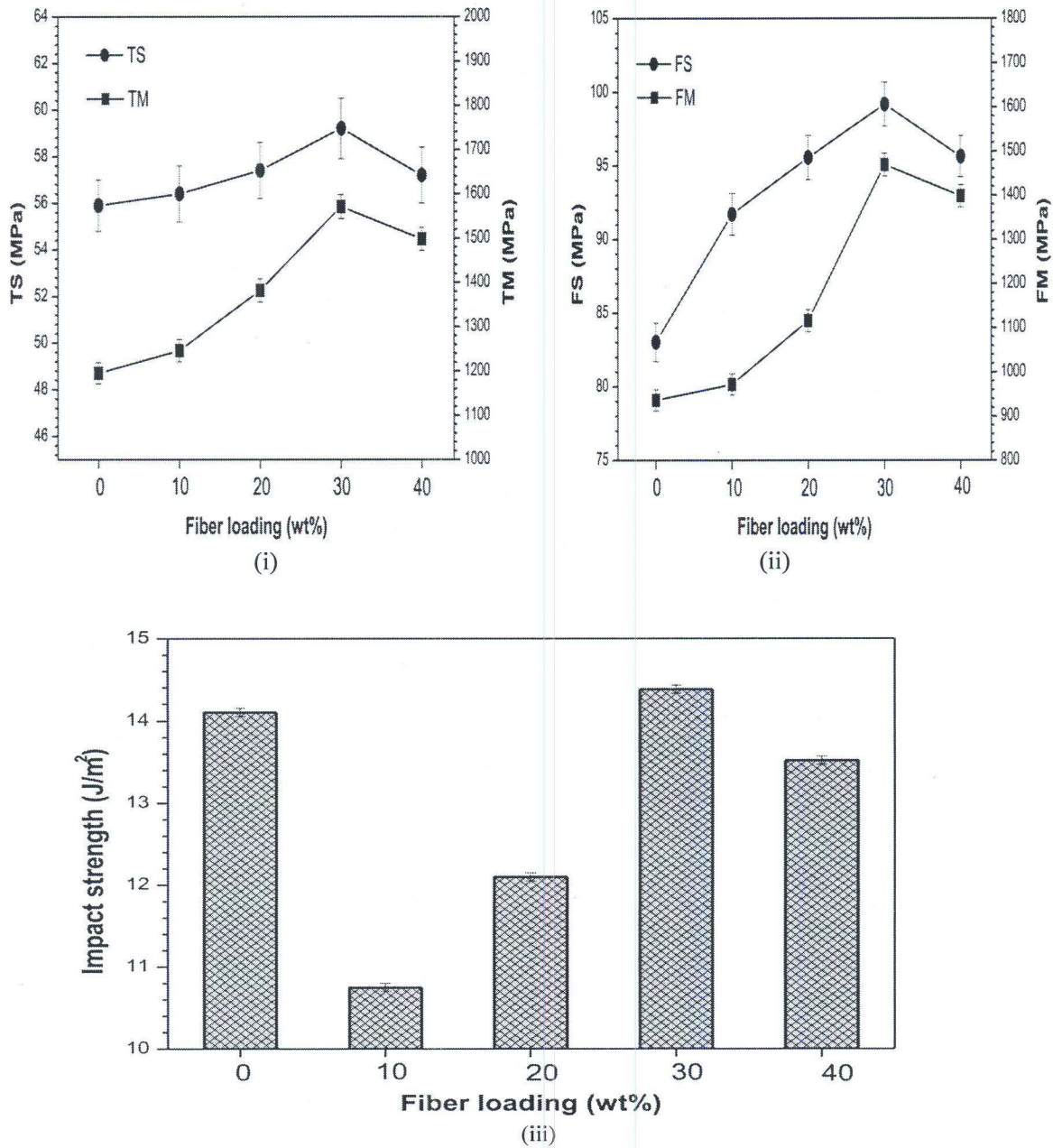


Fig. 3. Effect of fiber loading on mechanical properties of untreated oil palm empty fruit bunch fiber and PLA (OPEFB/PLA) composite

Fig. 4i, ii and iii represents the comparison of mechanical properties between pure PLA, untreated fiber composite (UFC) and treated fiber composite (TFC). The values are TS of 55.9, 59.2 and 73.1 MPa, TM of 1195, 1571 and 2099 MPa, FS of 83, 99, and 116 MPa, FM of 936, 1469 and 1758 MPa and IS of 14.1, 14.4 and 16.2 J/m² respectively for PLA, UFC and TFC. Clearly, it can be seen that treated fiber composites produced the highest mechanical properties. The enhancement in properties of TFC over UFC are 23.5%, 33.6%, 16.8%, 19.6% and 13% respectively for TS, TM, FS, FM and IS. These figures denote

reasonable values to enhance materials properties and selection. The improved performance of TFC over UFC can be associated with increased fiber-matrix interfacial adhesion (Moshiul Alam et al., 2012). This enhancement was about by effective delignification of OPEFB fibers through the cavitation effect of ultrasound treatment on the fibers in alkali medium. A comprehensive mechanism for lignin and other non-cellulosic components removal from OPEFB fiber with respect to treatment can be found in literature (Chowdhury et al., 2013). The improved fiber-matrix interfacial adhesion therefore led to effective stress transfer between the PLA matrix and OPEFB fiber, and invariably produced composites with improved mechanical properties, as also reported elsewhere (Ochi, 2008).

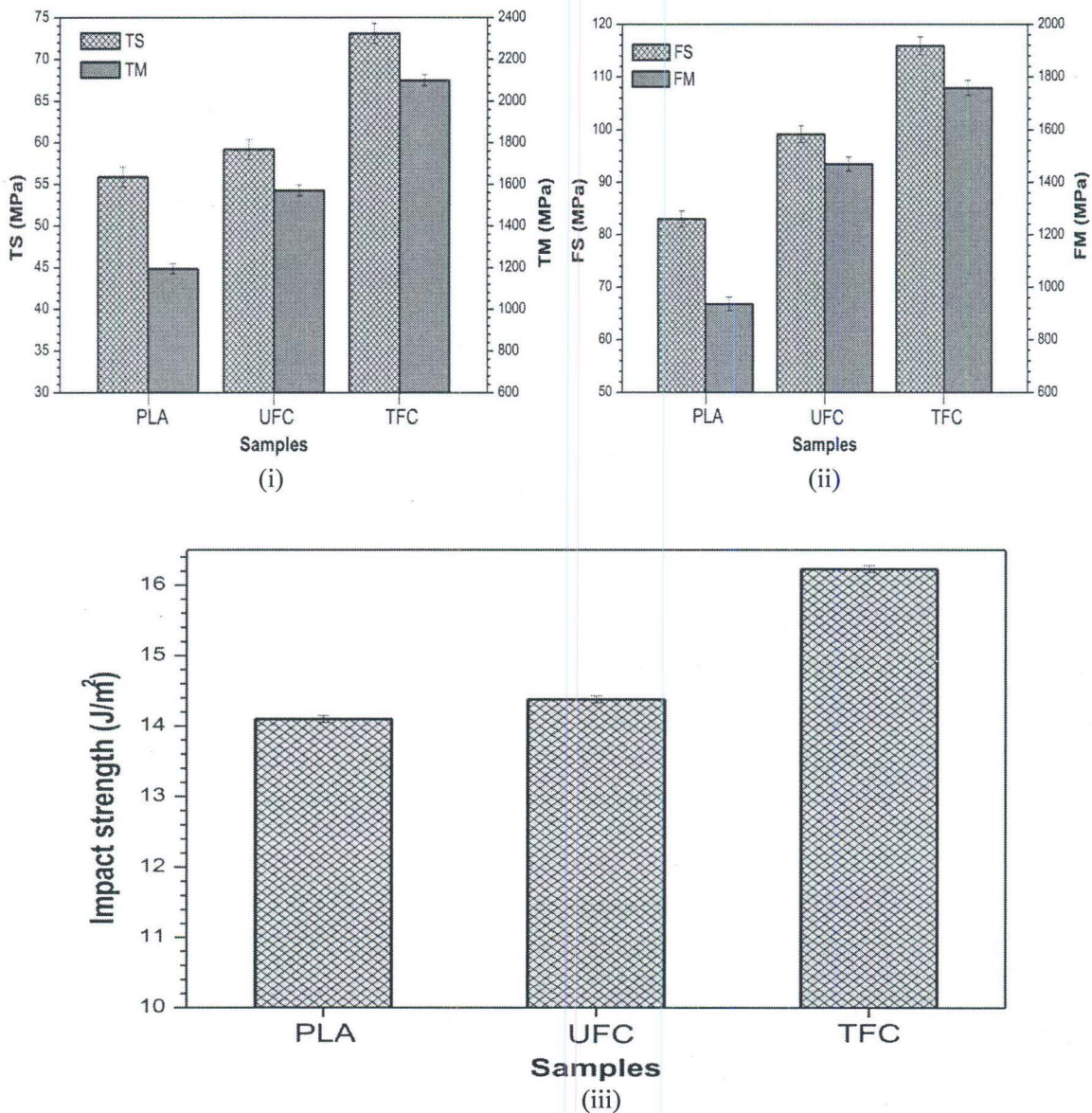


Fig. 4. Comparison of (i) TS, TM (ii) FS, FM and (iii) IS of pure PLA, untreated OPEFB fiber composite (UFC) and treated OPEFB fiber composite (TFC).

Thermal stability of composites

The TGA and DTG curves for PLA, UFC and TFC are presented in Fig. 5i and ii. From the curve in 5i, thermal degradation of pure PLA can be seen to be in one stage, showing an observable onset of weight-loss from 320-385°C. On the other hand for the composites, the degradation can be seen to begin at a lower temperature when compared with PLA. The initial drop observed around 98°C for the composites, could be due to result of release of absorbed moisture. Moreover, there is a conspicuous difference between the sudden drop that occurred around 290°C for composites and that of pure PLA. Also, two temperature ranges of 285-385°C and 385-490°C were noticed for the composites which may be accrued to the thermal decomposition feature of the OPEFB fiber molecules in the composites. Although the degradation temperature (T_d) can be obtained from the DTG data plotted in Figure 5ii, degradation temperature of a sample at 50% weight loss is usually considered as an indicator for its structural destabilization (Chowdhury et al., 2013). The T_d values evaluated for PLA, UFC and TFC are 364°C, 322°C and 340°C respectively whereas the corresponding weight losses are 67.64%, 61.65% and 49.76% respectively. This suggests that ultrasound and alkali treatment of OPEFB fibers could increase the effectiveness of the fiber to restrict the mobility of macromolecular chains of PLA matrix, through improved surface interaction. The implication of effective macromolecular chain restriction therefore would mean an increased thermal stability (Awal, Ghosh, & Sain, 2010; Lee et al., 2009).

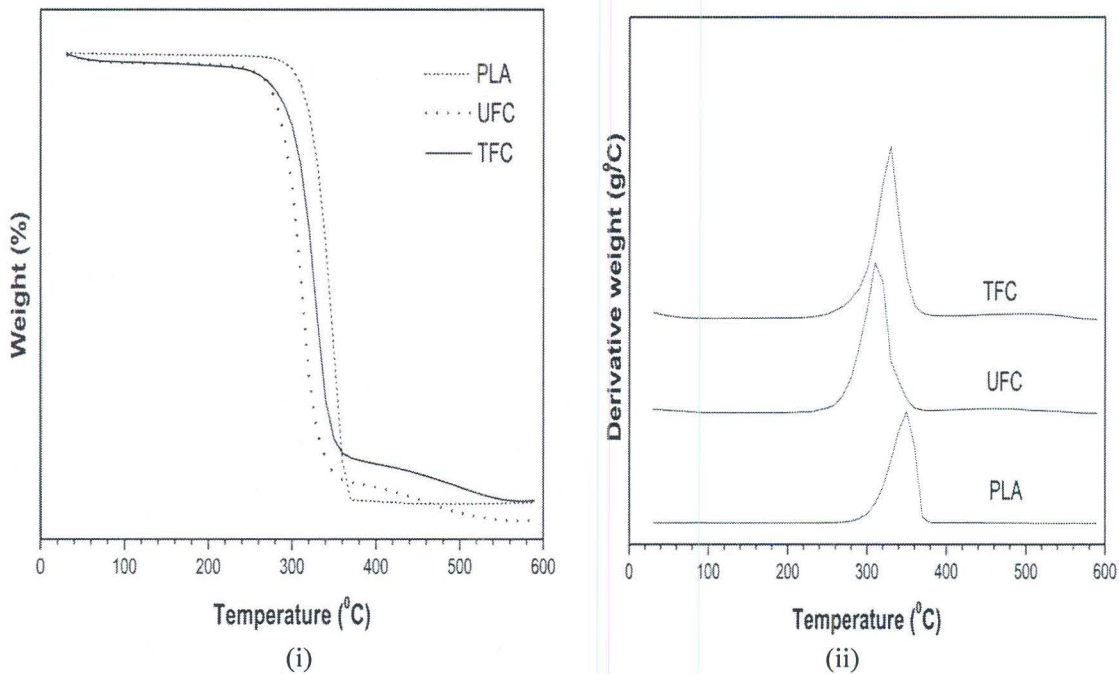


Fig. 5. TGA and DTG curves of pure PLA, untreated OPEFB fiber composite (UFC) and treated OPEFB fiber composite (TFC).

4. CONCLUSION

Treatment of OPEFB fibers with ultrasound in alkali medium of low concentration was able to produce considerable modifications to the fiber morphological functional and structural properties.

Inclusion of ultrasound treated OPEFB fiber into PLA matrix led to production of composites with highly desirable mechanical, structural and thermal properties especially when compared with pure PLA and also untreated fiber composites. The improvement in mechanical properties of treated fiber composites over untreated fiber composites is 23.5%, 33.6%, 16.8%, 19.6% and 13% for TS, TM, FS, FM and IS respectively. Thus ultrasound treatment of OPEFB fibers led to better improved properties as well as reasonable enhancement to the treated fiber reinforced PLA composite.

ACKNOWLEDGEMENT

The authors would like to appreciate the Malaysia Ministry of Education for the financial support of this project through FRGS (RDU120106), and University Malaysia Pahang for providing PGRS grant through (GRS140343).

REFERENCES

- Aimin, T., Hongwei, Z., Gang, C., Guohui, X., & Wenzhi, L. (2005). Influence of ultrasound treatment on accessibility and regioselective oxidation reactivity of cellulose. *Ultrasonics sonochemistry*, 12(6), 467-472.
- Awal, A., Ghosh, S., & Sain, M. (2010). Thermal properties and spectral characterization of wood pulp reinforced bio-composite fibers. *Journal of thermal analysis and calorimetry*, 99(2), 695-701.
- Bledzki, A. K., Jaszkiwicz, A., & Scherzer, D. (2009). Mechanical properties of PLA composites with man-made cellulose and abaca fibres. *Composites Part A: Applied Science and Manufacturing*, 40(4), 404-412.
- Bledzki, A. K., Mamun, A. A., & Feldmann, M. (2012). Polyoxymethylene composites with natural and cellulose fibres: Toughness and heat deflection temperature. *Composites Science and Technology*, 72(15), 1870-1874.
- Chowdhury, M., Beg, M., Khan, M. R., & Mina, M. (2013). Modification of oil palm empty fruit bunch fibers by nanoparticle impregnation and alkali treatment. *Cellulose*, 20(3), 1477-1490.
- Goriparthi, B. K., Suman, K., & Mohan Rao, N. (2012). Effect of fiber surface treatments on mechanical and abrasive wear performance of polylactide/jute composites. *Composites Part A: Applied Science and Manufacturing*, 43(10), 1800-1808.
- Huda, M. S., Drzal, L. T., Mohanty, A. K., & Misra, M. (2008). Effect of fiber surface-treatments on the properties of laminated biocomposites from poly (lactic acid)(PLA) and kenaf fibers. *Composites Science and Technology*, 68(2), 424-432.
- Islam, M., Beg, M., Gupta, A., & Mina, M. (2013). Optimal performances of ultrasound treated kenaf fiber reinforced recycled polypropylene composites as demonstrated by response surface method. *Journal of Applied Polymer Science*, 128(5), 2847-2856.
- Joseph, S., Joseph, K., & Thomas, S. (2006). Green composites from natural rubber and oil palm fiber: physical and mechanical properties. *International Journal of Polymeric Materials*, 55(11), 925-945.
- Khalid, M., Salmiaton, A., Chuah, T., Ratnam, C., & Choong, S. T. (2008). Effect of MAPP and TMPTA as compatibilizer on the mechanical properties of cellulose and oil palm fiber empty fruit bunch-polypropylene biocomposites. *Composite Interfaces*, 15(2-3), 251-262.
- Lee, B.-H., Kim, H.-S., Lee, S., Kim, H.-J., & Dorgan, J. R. (2009). Bio-composites of kenaf fibers in polylactide: Role of improved interfacial adhesion in the carding process. *Composites Science and Technology*, 69(15), 2573-2579.
- Mamun, A. A., Heim, H.-P., Beg, D. H., Kim, T. S., & Ahmad, S. H. (2013). PLA and PP composites with enzyme modified oil palm fibre: A comparative study. *Composites Part A: Applied Science and Manufacturing*, 53, 160-167.
- Meon, M. S., Othman, M. F., Husain, H., Remeli, M. F., & Syawal, M. S. M. (2012). Improving tensile properties of kenaf fibers treated with sodium hydroxide. *Procedia Engineering*, 41, 1587-1592.

- Mohanty, S., Verma, S. K., Nayak, S. K., & Tripathy, S. S. (2004). Influence of fiber treatment on the performance of sisal–polypropylene composites. *Journal of Applied Polymer Science*, 94(3), 1336-1345.
- Moshiul Alam, A., Beg, M., Reddy Prasad, D., Khan, M., & Mina, M. (2012). Structures and performances of simultaneous ultrasound and alkali treated oil palm empty fruit bunch fiber reinforced poly (lactic acid) composites. *Composites Part A: Applied Science and Manufacturing*, 43(11), 1921-1929.
- Müller, C. M., Laurindo, J. B., & Yamashita, F. (2009). Effect of cellulose fibers on the crystallinity and mechanical properties of starch-based films at different relative humidity values. *Carbohydrate Polymers*, 77(2), 293-299.
- Muthukumar, S., Kentish, S. E., Stevens, G. W., & Ashokkumar, M. (2006). Application of ultrasound in membrane separation processes: a review. *Reviews in chemical engineering*, 22(3), 155-194.
- Ochi, S. (2008). Mechanical properties of kenaf fibers and kenaf/PLA composites. *Mechanics of materials*, 40(4), 446-452.
- Petersson, L., Kvien, I., & Oksman, K. (2007). Structure and thermal properties of poly (lactic acid)/cellulose whiskers nanocomposite materials. *Composites Science and Technology*, 67(11), 2535-2544.
- Pickering, K. L., Sawpan, M. A., Jayaraman, J., & Fernyhough, A. (2011). Influence of loading rate, alkali fibre treatment and crystallinity on fracture toughness of random short hemp fibre reinforced polylactide bio-composites. *Composites Part A: Applied Science and Manufacturing*, 42(9), 1148-1156.
- Sgriccia, N., Hawley, M., & Misra, M. (2008). Characterization of natural fiber surfaces and natural fiber composites. *Composites Part A: Applied Science and Manufacturing*, 39(10), 1632-1637.
- Sun, R., Tomkinson, J., & Ye, J. (2003). Physico-chemical and structural characterization of residual lignins isolated with TAED activated peroxide from ultrasound irradiated and alkali pre-treated wheat straw. *Polymer degradation and stability*, 79(2), 241-251.
- Wirjosentono, B., Guritno, P., & Ismail, H. (2004). Oil palm empty fruit bunch filled polypropylene composites. *International Journal of Polymeric Materials*, 53(4), 295-306.
- Zhou, Z., Liu, X., Hu, B., Wang, J., Xin, D., Wang, Z., & Qiu, Y. (2011). Hydrophobic surface modification of ramie fibers with ethanol pretreatment and atmospheric pressure plasma treatment. *Surface and Coatings Technology*, 205(17), 4205-4210.